Giant magneto-impedance effects in nanocrystalline soft magnetic alloy ribbons

KU Wanjun[1], GE Fuding[1], YAN Ge[1], WANG Xinyan[1] and ZHU Jing[2]

1. Central Iron and Steel Research Institute, Beijing 100081; 2. Department of Materials Science and Engineering, Tsinghua University, Beijing 100084, China

Keywords: giant magneto-impedance effects (GMI), magnetic permeability, penetration depth, nanocrystalline soft magnetic alloy ribbon.

SINCE the discovery of the giant magneto-impedance (GMI) effects in amorphous wire (or ribbon) of CoFeSiB and nanocrystalline wire (or film) of FeCuNbSiB[1—4], it has attracted great attention due to its promising potential applications in industry. Amorphous (and nanocrystalline) soft magnetic alloys have very large magnetic permeability, when an ac driving current and an external magnetic field (EMF) are applied, the EMF will damp the magnetic flux change caused by the ac driving current, thus the magnetic permeability will decrease; as a result, the penetration depth will increase, hence the impedance, $Z = R + jX$, of the specimen will decrease, finally resulting in GMI (R, X, Z) effects[5, 6]. Nanocrystalline structure will form in alloys, such as $Fe_{73.5}Cu_1T_3Si_{13.5}B_9$ (T = Nb, Mo) and $Fe_{79.5}P_{12}C_6Cu_{0.5}Mo_{0.5}$-$Si_{1.5}$. When annealed at proper temperatures, the nanocrystalline structure can decrease the magnetic anisotropy field and magnetostriction constant, thus increasing the permeability[7, 8]. In this note, the above-mentioned three kinds of amorphous alloys were first annealed, then GMI effects in these alloys were examined as functions of the EMF and the driving current frequencies, and the origin of GMI was discussed. Here GMI is defined as GMI(R, X, Z) = [R, X, Z(Hex) − R, X, Z(0)]/R, X, Z(0) × 100%.

1 Experimental

Ribbons of $Fe_{73.5}Cu_1Nb_3Si_{13.5}B_9$, 15 mm wide and 40 μm thick, $Fe_{73.5}Cu_1Mo_3Si_{13.5}B_9$, 15 mm wide and 25 μm thick, $Fe_{79.5}P_{12}C_6Cu_{0.5}Mo_{0.5}Si_{1.5}$, 10 mm wide and 30 μm thick, were made through the single roller rapid quenching. In order to measure GMI, specimens 20 mm long and 3 mm wide were cut off from the ribbons. The $Fe_{73.5}PCu_1Nb_3Si_{13.5}B_9$ was annealed at 823 K for 1 h, $Fe_{73.5}Cu_1Mo_3Si_{13.5}B_9$ at 793 K for 1 h and $Fe_{79.5}P_{12}C_6Cu_{0.5}Mo_{0.5}Si_{1.5}$ at 653 K for 0.5 h. The impedance was usually measured by the four-terminal methods using an HP4192A impedance analyzer. The EMF was applied by a solenoid. During the measurement, the EMF and the driving current, parallel to each other, were kept on the specimen plane.

2 Results and discussion

Figure 1 shows that GMI(R) first increases with frequency from a small value, reaching the maximum at about 5 MHz, then it begins to decrease so slowly that it almost cannot be detected, while GMI(X) decrease quickly, and GMI(Z) first increases quickly to the maximum then decreases. At low frequency, it is the change of GMI(X) that dominates the change of GMI(Z) while at high frequency it is the change of GMI(R) that dominates the change of GMI(Z). At 0.7 MHz, GMI(Z) shows its maximum value which is about 42%. We can also find that when GMI(R) equals GMI(X), GMI(Z) shows its maximum value.

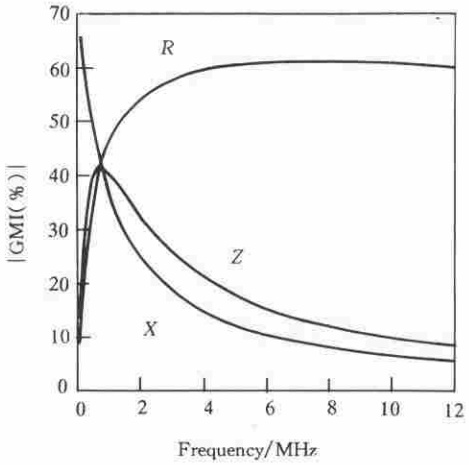

Fig. 1. Variation of GMI(R, X, Z) as a function of the ac driving current frequency (f) for the nanocrystalline $Fe_{73.5}Cu_1Nb_3Si_{13.5}B_9$ alloy ribbon. EMF, 12O Oe (9.55 kA/m); driving current, 10 mA.

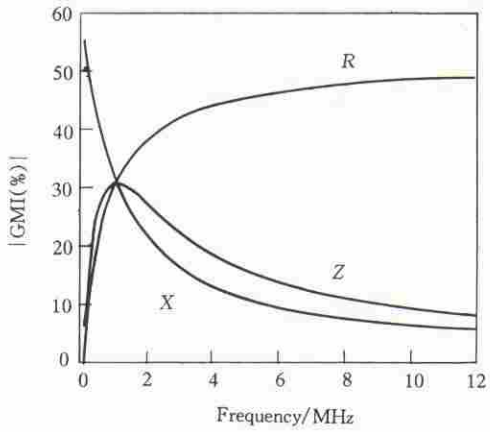

Fig. 2. Variation of GMI(R, X, Z) as a function of the ac driving current frequency (f) for the nanocrystalline $Fe_{73.5}Cu_1Mo_3Si_{13.5}B_9$ alloy ribbon. EMF, 110 Oe (8.76 kA/m); driving currant, 10 mA.

Figure 2 shows the same behavior as in fig. 1. When the frequency is 1.0 MHz, GMI(Z) shows its maximum value, ——31%.

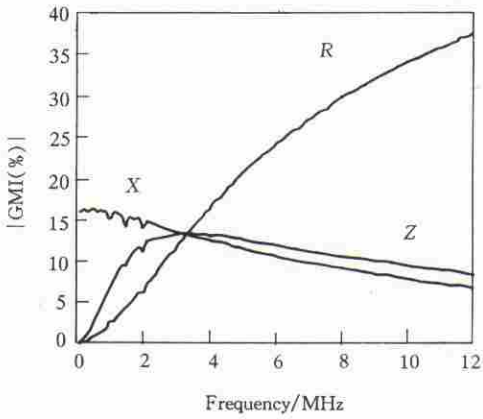

Fig. 3. Variation of GMI(R, X, Z) as a function of the ac driving current frequency (f) for the nanocrystalline $Fe_{79.5}P_{12}C_6Cu_{0.5}Mo_{0.5}Si_{1.5}$ alloy ribbon. EMF, 100 Oe (8 kA/m); driving current, 10 mA.

Figure 3 shows that when the frequency is 3.3 MHz, GMI(Z) reaches its maximum value, ——13.3%.

According to Landau *et al.*[9] and Panina *et al.*[10], at different frequencies, the impedance shows different characteristics: at low frequency, the skin effects of the ac driving current is very weak, the imaginary part of the impedance $Z = R + iX$, X, is proportional to the initial permeability of the specimen, the EMF damps the change of the transverse magnetic flux, decreases the permeability to a very low value, thus decreasing the impedance and leading to the giant change of X with the application of the external field. With the increase of frequency, the skin effect becomes much obvious, the flux change will become small with the same external field, leading to the decrease of GMI(X). At much higher frequency, due to the increase of classic eddy loss and anomalous eddy loss caused by the move of domain wall, the external field makes the permeability decrease, hence leading to the giant change of the real part, R, of impedance Z. At a certain frequency, when GMI(R) is almost equal to GMI(X), GMI(Z) reaches its maximum value. GMI(Z) can be improved by the decrease of the dc current resistance of the ribbon, the change of domain structure and the increase of permeability.

The permeability of the specimen depends on not only the external field but also the

anisotropy field in the specimen. With the increase of the frequency, compared to the external field, the effects of the local surface anisotropy field becomes much obvious due to the development of skin effects; this is the reason why GMI(R) in $Fe_{73.5}Cu_1Nb_3Si_{13.5}$-$B_9$ decreases at high frequency. Comparing the GMI(Z) of the three specimens, it can be found that $Fe_{73.5}Cu_1Nb_3Si_{13.5}B_9$ shows the highest value, because the permeability of $Fe_{73.5}Cu_1Nb_3Si_{13.5}B_9$ is the highest and the most sensitive one to the external field. It can also be seen that the GMI(Z) peak of $Fe_{79.5}P_{12}C_6Cu_{0.5}Mo_{0.5}Si_{1.5}$ is very broad, suggesting the complex distribution of the anisotropy field. Because the permeability of $Fe_{79.5}P_{12}C_6Cu_{0.5}Mo_{0.5}Si_{1.5}$ is the lowest one of the three specimens, it is the least sensitive to the external field. Therefore the increase of GMI(Z) with frequency is very slow.

Figures 4—6 show the external field dependence of the GMI(R, X, Z) effects in the three specimens, respectively, with frequency fixed at 1 MHz and the driving current at 10 mA. The figures show that it is easy for the GMI(R, X, Z) effects of $Fe_{73.5}Cu_1Nb_3Si_{13.5}B_9$ to become saturated with the increase of the external field while it is difficult to saturate $Fe_{79.5}P_{12}C_6Cu_{0.5}$-$Mo_{0.5}Si_{1.5}$. For example, when the external field is 0.8 kA/m (10 Oe), GMI (Z) of $Fe_{73.5}$-$Cu_1Nb_3Si_{13.5}B_9$ is about 15% while it is only about 3% for $Fe_{79.5}P_{12}C_6Cu_{0.5}Nb_{0.5}Si_{1.5}$, and

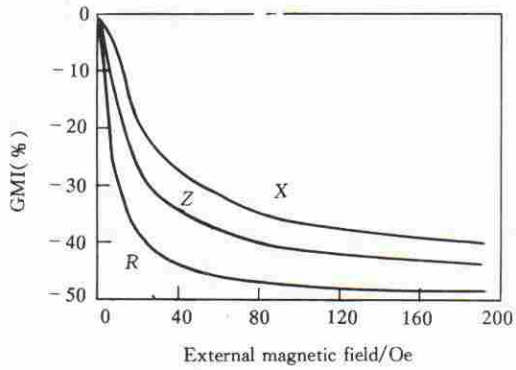

Fig. 4. GMI(R, X, Z) correlates with EMF for the nanocrystalline $Fe_{73.5}Cu_1Nb_3Si_{13.5}B_9$ alloy ribbon with a fixed ac driving current frequency of 1 MHz.

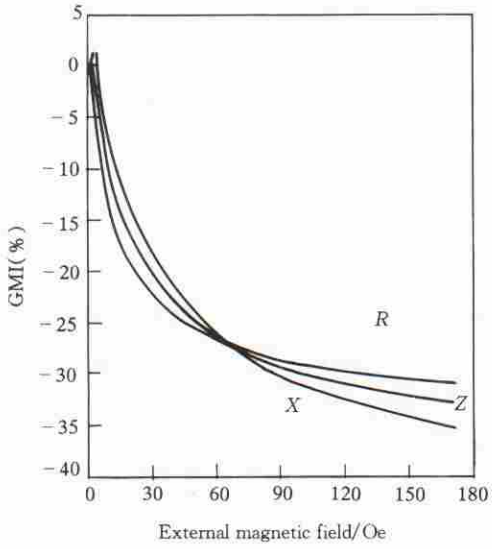

Fig. 5. GMI(R, X, Z) correlates with EMF for the nanocrystalline $Fe_{73.5}Cu_1Mo_3Si_{13.5}B_9$ alloy ribbon with a fixed ac driving current frequency of 1 MHz.

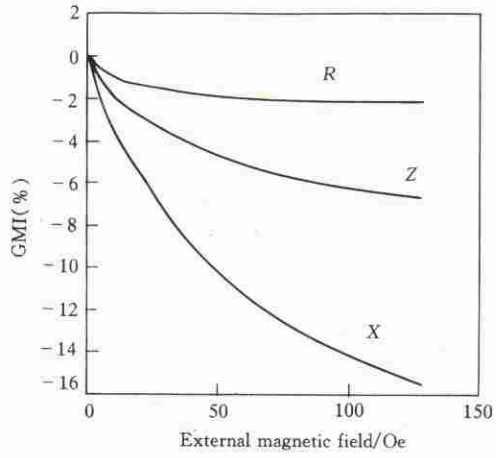

Fig. 6. GMI(R, X, Z) correlates with EMF for the nanocrystalline $Fe_{79.5}P_{12}C_6Cu_{0.5}Mo_{0.5}Si_{1.5}$ alloy ribbon with a fixed ac driving current frequency of 1 MHz.

about 10% for $Fe_{73.5}Cu_1Mo_3Si_{13.5}B_9$ in the middle of $Fe_{73.5}Cu_1Nb_3Si_{13.5}B_9$ and $Fe_{79.5}P_{12}C_6Cu_{0.5}Mo_{0.5}Si_{1.5}$. The reason is that the two-phase structure of α-FeSi (or α-Fe) and residual amorphous matrix formed in annealed $Fe_{73.5}Cu_1T_3Si_{13.5}B_9$ (T = Nb, Mo) and $Fe_{79.5}P_{12}C_6Cu_{0.5}Mo_{0.5}Si_{1.5}$, leading to a decrease in anisotropy field, the anisotropy field in $Fe_{73.5}Cu_1Nb_3Si_{13.5}B_9$ is the lowest, hence GMI can be saturated with a small external field, which makes it more suitable for practical applications.

In summary, in order to make the specimen show high GMI with a small external field, it is necessary to decrease its anisotropy field and improving its distribution, thus improve its permeability. Further, by decreasing the resistivity of the alloys, great classic eddy loss can be achieved at a small driving current frequency, then at a proper frequency, both GMI(R) and GMI(X) show high values; as a result, GMI(Z) is improved.

(*Received September* 26, 1996)

References

1 Mandal, K., Ghatak, S. K., Large magnetoresistance in an amorphous $Co_{68.1}Fe_{4.4}Si_{12.5}B_{15}$ ferromagnetic wire, *Phys. Rev.*, B, 1993, 47(21): 14233.
2 Mohri, K., Kohzawa, T., Kawashima, K. *et al.*, Magneto-inductive effect (MI effect) in amorphous wires, *IEEE Trans. Magn.*, 1992, 28(5): 3150.
3 Sommer, R. L., Chien, L. C., Longitudinal and transverse magneto-impedance in amorphous $Fe_{73.5}Cu_1Nb_3Si_{13.5}B_9$ films, *Appl. Phy. Lett.*, 1995, 67(22): 3346.
4 Knobel, M. Sánchez, M. L., Marin, P. *et al.*, Influence of nanocrystallization on the magneto-impedance effect in Fe-CuNbSiB amorphous wires, *IEEE Trans. Magn.*, 1995, 31(6): 4009.
5 Costa-Krämer, J. L. S., Rao, K. V., Influence of magnetostriction on magneto-impedance in amorphous soft ferromagnetic wires, *IEEE Trans. Magn.*, 1995, 31(2): 1261.
6 Panina, L. V., Mohri, K., Uchiyama, T. *et al.*, Giant magneto-impedance in Co-rich amorphous wires and films, *IEEE Trans. Magn.*, 1995, 31(2): 1249.
7 Herzer, G., Effects of magnetic field annealing on magnetic properties in ultrafine crystalline Fe-Cu-Nb-Si-B alloys, *IEEE Trans Magn.*, 1989, 25(5): 3324—3326.
8 Fujii, Y., Fujita, H., Seki, A. *et al.*, Magnetic properties of fine crystalline Fe-P-C-Cu-X alloys, *J. Appl. Phys.*, 1991, 70(10): 6241.
9 Landau, L. D., Lifshitz, E. M., *Electrodynamics of Continuous Media*, Oxford: Pergamon Press, 1975, 195.
10 Panina, L. V., Mohri, K., Magneto-impedance effect in amorphous wires, *Appl. Phys. Lett.*, 1994, 65(9): 1189.

Acknowledgement Thanks are due to Prof. Wang Xinlin and Zhang Chuanli for their kind support and encouragement. This work was supported by National Natural Science Foundation (Grant No. 49472149) and Foundation of Ministry of Metallurgical Industry.

Raman studies on the crystallization of sol-gel processed $PbTiO_3$ thin films

ZHU Tao[1], HAN Gaorong[1], HAN Zhengfu[2] and DING Zishang[1]

1. Department of Materials Science and Engineering, Zhejiang University, Hangzhou 310027, China; 2. State Key Synchrotron Radiation Laboratory, University of Science and Technology of China, Hefei 230026, China

Keywords: Raman spectra, $PbTiO_3$ thin films, sol-gel process.

$PbTiO_3$ thin films are of interest to a number of device applications as IR detectors, ultrasonic transducers, etc. Early work on the fabrication of $PbTiO_3$ thin film was mainly based on rf sputtering[1]. Recently, sol-gel processing has been gaining interest in the production of